

## Article

# Three-Dimensional Modeling of Soil-Structure Interaction for a Bridge Founded on Caissons under Seismic Conditions

Davide Pauselli \*, Diana Salciarini  and Filippo Ubertini 

Department of Civil and Environmental Engineering, University of Perugia, 06125 Perugia, Italy

\* Correspondence: [davide.pauselli@studenti.unipg.it](mailto:davide.pauselli@studenti.unipg.it)

**Abstract:** In recent years, the urgent need to increase the safety standards of viaducts and bridges—under static and dynamic loading conditions—has required the development of advanced modeling approaches able to accurately predict the expected behavior of such infrastructures in a reliable manner. This paper presents a comparison between the adoption of a simplified modeling approach, widely used in the current practice, where the response of the structural system neglects the effects of the soil-structure interaction (SSI) phenomenon (considering the base of the structure fixed at the ground surface) and a rigorous modeling approach that considers the full 3D problem with all the components of the system (superstructure, foundation, and soil), through a finite element model. The pier of a real-world viaduct in central Italy was considered, with the aim of starting from a specific case study with foundation characteristics that are frequently found in viaducts in Italy, to obtain results that can be generalized to a wide range of similar types. Its behavior was evaluated both in the dynamic range of small oscillations and in the field of the seismic response to low and strong motion events. The results show that, in terms of seismic demand, the fixed-based model appears more conservative, but it significantly underestimates both elastic and residual displacements and rotations



**Citation:** Pauselli, D.; Salciarini, D.; Ubertini, F. Three-Dimensional Modeling of Soil-Structure Interaction for a Bridge Founded on Caissons under Seismic Conditions.

*Appl. Sci.* **2022**, *12*, 10904.  
<https://doi.org/10.3390/app122110904>

Academic Editor: Arcady Dyskin

Received: 28 September 2022

Accepted: 21 October 2022

Published: 27 October 2022

**Publisher's Note:** MDPI stays neutral with regard to jurisdictional claims in published maps and institutional affiliations.



**Copyright:** © 2022 by the authors. Licensee MDPI, Basel, Switzerland. This article is an open access article distributed under the terms and conditions of the Creative Commons Attribution (CC BY) license (<https://creativecommons.org/licenses/by/4.0/>).

**Keywords:** soil-structure interaction; seismic response; strong motion; deep foundations; viaduct

## 1. Introduction

The use of reliable behavioral models for bridges and viaducts is the fulcrum for both the design of new infrastructures and safety assessment of existing ones. Very often, the viaduct piers are founded on deep foundations, such as piles or caissons, to transmit the structural loads to deeper soil layers characterized by enhanced mechanical properties. As found by previous studies [1–5], a concrete caisson is characterized by a significant stiffness contrast with respect to the surrounding soil, and its massive volume constitutes a major portion of the weight of the entire viaduct structure. Consequently, the seismic behavior of viaducts can be strongly influenced by the response of the foundation system, and in a seismic analysis, proper caisson modeling is of pivotal importance to evaluate its effect on the superstructure.

The influence of the Soil-foundation Structure Interaction (SSI) phenomenon on the dynamic response of relatively flexible structures characterized by isolated foundations has been extensively studied in the last decades [6–12]. A proper schematization of the SSI includes: (i) the interpretation of the modal properties of the bridges as identified through operational modal analysis [13,14], (ii) their estimated state of health (field of Structural Health Monitoring (SHM)) [15], and (iii) the prediction of the dynamic response to the occurrence of medium/high-intensity seismic phenomena [16–20]. In general, the SSI problem shows a high level of complexity: by definition, it is a coupled problem in which the action strongly depends on the reaction of the structural system [21]. Although EN 1998-5 seismic code states that the effects of SSI under dynamic conditions have to be considered for structures with massive and deep foundations, most of the structural design

and assessment procedures adopt the assumption that the structural elements are fixed to the ground preventing translation and rotation, as highlighted in the introduction of several recent studies [1,22–24] that show the improved modeled response of structures when SSI is modeled. In general, the static and, especially, dynamic structural responses are strongly influenced by the stiffness relationships between the superstructure, the foundation, and the ground. Thus, ignoring the effects of the SSI phenomena can lead to relevant errors in the evaluation of the structural response under dynamic loads. A clear understanding of the relevance of this error still deserves more investigations for different foundation types and boundary conditions, despite it being well known that it depends on several parameters, such as stiffness ratio between soil and structure, structure slenderness, and seismic input characteristics [2,3,5,10,11]. This paper aims to provide a further contribution to knowledge by studying a specific case of a stocky foundation (caisson) resting on a relatively stiff soil layer, and by exploring the importance of the SSI effect when the structure is loaded with different seismic inputs.

The approaches for the SSI analysis are classified into direct and indirect methods, as reported, for example, by [25,26]. Among the indirect methods, the most widespread one addresses the SSI problem by an uncoupled approach (“substructure method”) in which the superstructure analysis is solved independently from the soil–caisson system. The SSI problem is determined independently by separating the effects caused by the kinematic interaction from those caused by inertial interaction. The response of the overall system is then obtained through the application of the principle of superposition of effects [25]. The inertial interaction is solved by a series of (visco-)elastic elements—one for each degree of freedom of the system—whose stiffness and damping coefficients are defined through equivalent springs and dashpots [10–12]. This approach does not consider the possible coupling between the different degrees of freedom and the inelastic response induced by plastic deformations which might develop in the foundation soil even under relatively low loading conditions [27,28]. Surrogate implementations in the time domain for inertial SSI can also include masses, leading to the well-known monkey tail approach [29]. Other pioneering works on the topic were conducted by [30,31].

Among the simplified approaches, a possible alternative to correctly consider the effects of nonlinearities in SSI problems is based on the concept of *macro-element* where the entire foundation–soil system is schematized through a single point at the base of the superstructure (*lumped mass* model) with three or six degrees of freedom (respectively, for 2D or 3D problems). The first application of the macro element concept in geotechnical engineering is due to the contribution of Nova and Montrasio [32], who presented the formulation of a method to assess the settlements of a strip foundation on cohesionless soils subjected to quasi-static monotonic loading. Successive developments and applications of the concept of macro-elements applied to bridges founded on shallow foundations are due to [9,26,32–35], among others. Many applications demonstrated that this approach can be very effective in predicting the structural behavior under dynamic loading conditions [32–37], yet it requires a very detailed characterization of the soil parameters to properly calibrate all the variables included in the mathematical formulations.

In the direct approaches [25], the soil volume, the foundation, and the superstructure are part of the same model, analyzed together using numerical methods based on a continuum discretization of the domain (typically, by either the Finite Element Method, FEM, or the Finite Difference Method, FDM). Dynamic numerical analyses performed through FEM approaches can be very effective to analyze the seismic behavior of structures due to their ability to simulate complex geometry, boundary conditions, soil and structure dynamic behavior [38–41]. The crucial aspects to obtaining reliable predictions rely on the correct selection of the seismic input, proper adoption of domain discretization, and suitable choice of boundary conditions.

Following the direct approach described above, in this paper we present the main results of a full 3D FE modeling to assess the dynamic response of a bridge pier founded on a caisson subjected to seismic loads. These results are compared with those derived by a

simplified model, where the bridge pier is embedded at the base, neglecting the SSI effects. The analysis has been limited to a single pier considered isolated; this is motivated by the goal of providing evidence of the importance of the phenomena, without aiming at giving an exact and faithful evaluation of the structural safety of the case study.

The structure of the paper is the following: after the brief literature introduction of Section 1, the examined viaduct is presented in Section 2, describing its structural features and the main geotechnical characteristics of the foundation soil. In Section 3, the seismic inputs used in the dynamic analyses are presented, while in Section 4, details on the numerical models are given. In Section 5, the main outcomes of the model are discussed and, finally, in Section 6, some concluding remarks and perspectives are listed.

## 2. Study-Case

The selected study case is a viaduct of the Perugia-A1 motorway in the municipality of Perugia, in central Italy, built in the 80's. An aerial view including the considered sector of the viaduct is given in Figure 1, along with the plan view with the selected pier (blue circle).

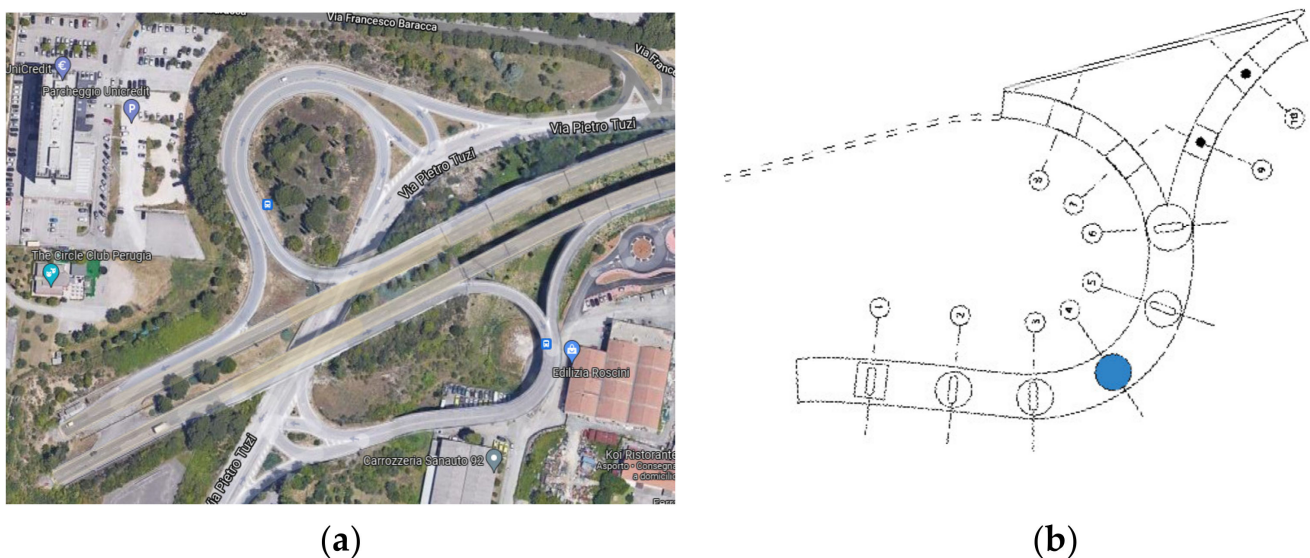


**Figure 1.** The figure shows: (a) the aerial view of the examined viaduct of the Perugia A1 motorway; and (b) the plan view of the considered sector where the blue circle indicates the considered pier (original project).

The viaduct is composed of eight piers of pseudo-rectangular cross-sections with a dimension of  $6 \times 2$  m; their lengths vary between 6 and 12 m, and the axial distance between each other is 19 m. The deck is constituted of a prestressed reinforced concrete hollow section, with a total weight of 4880 kN. The five central piers are founded on caissons of 8.3 m in diameter and 9 m in depth, while the three lateral (shorter) piers are founded on piled rafts. Figure 2 shows the longitudinal section of the viaduct derived from the original design plot (courtesy of National Autonomous Roads Corporation, ANAS). The soil stratigraphical information was obtained from the original project. The foundation soil is constituted of two layers: a first clayey layer—from the surface down to 9 m, and a fractured Marly formation—from 9 m to the end of the borehole (50 m). The depth of the water level is assumed at about 2 m from the ground surface, with small oscillations during the year. The base of the caissons reaches the Marly formation.

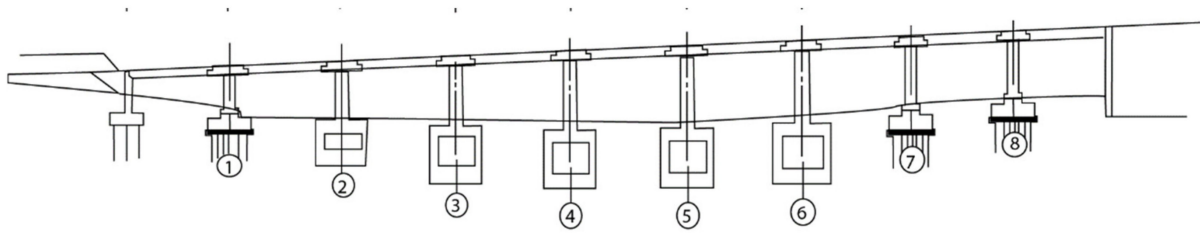


**Figure 2.** Longitudinal section of the examined viaduct, with the five (central) piers founded on caissons and the three (lateral) piers founded on piled rafts—sketch modified from the original project, 1981.

### 3. Seismic Input

A seismic input based on recorded, selected and scaled accelerograms was used for the dynamic analyses. This was defined using the REXEL code [42], which resorts to Italian or international databases. Starting from an elastic response spectrum target, the code produces a set of seven accelerograms satisfying spectrum-compatibility criteria. The code ensures that the selected records are compatible with: the local seismic-tectonic model, the earthquake magnitude, the magnitude and distance from the epicenter of (one or more) scenario events, the peak horizontal acceleration expected at the site, and the difference between the geotechnical properties at the seismic station and the construction site.

In this paper, we limited the presentation of the results to a single accelerogram, recorded during the Friuli earthquake (ID 00134y-Event 63), with a moment magnitude of 6.0 and epicentral distance of 14 km, and expected return time  $T_R = 950$  years. Figure 3 shows the seismic time history, its Fourier transform, and its pseudo-acceleration response spectrum with 5% damping, scaled to 1.5.

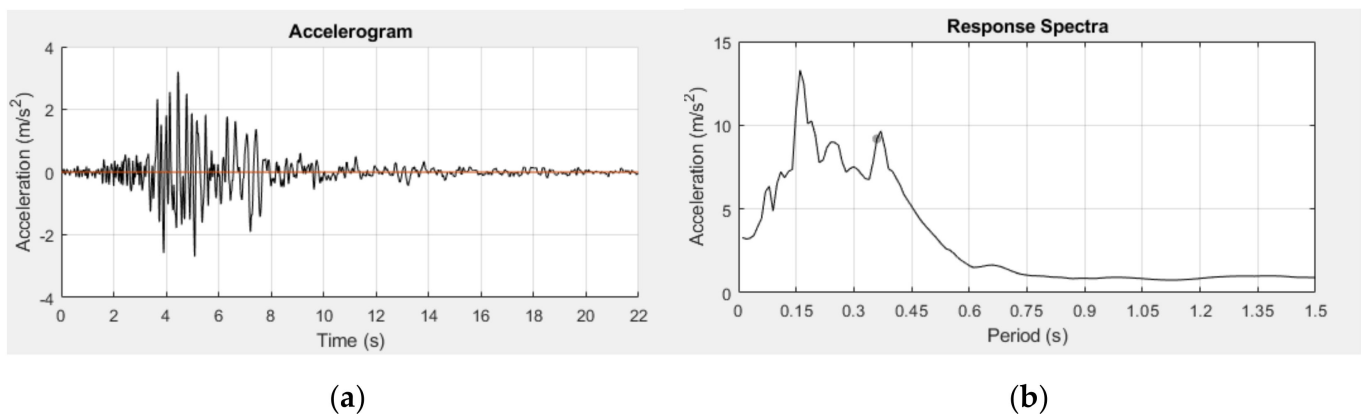


**Figure 3.** Seismic input n. 1 ( $F_a = 1.5$ ): (a) time history; (b) response spectrum.

The ID:00134y record was selected for its frequency distribution and relevant amplitude—deducible from the distance between the peak and the average frequency value. The seismic input was first scaled by a factor equal to 1.5 to obtain a high Arias Intensity,  $I_A$ , typical of strong motions. Then, it was scaled to 0.75 and 0.4 to explore the impact of weaker (but more frequent) input motions on the system response. Table 1 summarizes the main features of the four considered seismic inputs in terms of: scaling factor,  $F_a$ ; seismic duration,  $D$ ; peak ground acceleration, PGA; Arias Intensity,  $I_A$ ; peak frequency,  $f_{PEAK}$ ; mean frequency,  $f_{MEAN}$ ; mean period,  $T_{MEAN}$ ; and representative duration,  $D^*$ . The earthquake record was registered at outcropping bedrock, and it has a seismic duration  $D = 22$  s.

**Table 1.** Summary of the main features of the considered seismic inputs.

Code	Fa	D (s)	PGA	I <sub>A</sub> (cm/s)	f <sup>PEAK</sup> (Hz)	f <sup>MEAN</sup> (Hz)	T <sup>MEAN</sup> (s)	D* (s)
n. 1	1.5	44.17	0.326	0.87	2.66	4.48	0.304	4.609
n. 2	1.0	44.17	0.214	0.37	2.66	4.48	0.304	4.609
n. 3	0.75	44.17	0.163	0.21	2.66	4.48	0.304	4.609
n. 4	0.4	44.17	0.086	0.06	2.66	4.48	0.304	4.609

### 4. Numerical Modeling

To assess the seismic behavior of the central pier of the considered viaduct, and compare the different responses obtained by including or ignoring deformable soil, two different numerical models were developed: (i) an FE model of the pier perfectly embedded to the ground using the SAP2000 code [43], which ignores the SSI; and, (ii) a 3D FE model of the pier and the foundation soil using the PLAXIS 3D code [44], which considers the SSI effects. For both the models, the following analyses have been performed:

- Application of a lumped load at the top of the pier (in the direction of the system’s highest stiffness, i.e., orthogonal with respect to the deck direction) and analysis of the system free vibration, to determine the structure’s natural frequency at small strains;
- Application of the selected earthquake in the direction of the system’s highest stiffness (orthogonal with respect to the deck direction) and dynamic analysis of the system response.

In both the FE models described above, the ground surface has been considered horizontal and the mutual interaction between the piers has been ignored by assuming the loading condition orthogonal to the deck.

#### 4.1. SAP Model

The 3D FE model built with SAP2000 is shown in Figure 4a. The model is constituted of a Timoshenko linear visco-elastic beam element fixed at the base representing the pier of the bridge, with a 5% of Rayleigh damping ratio.

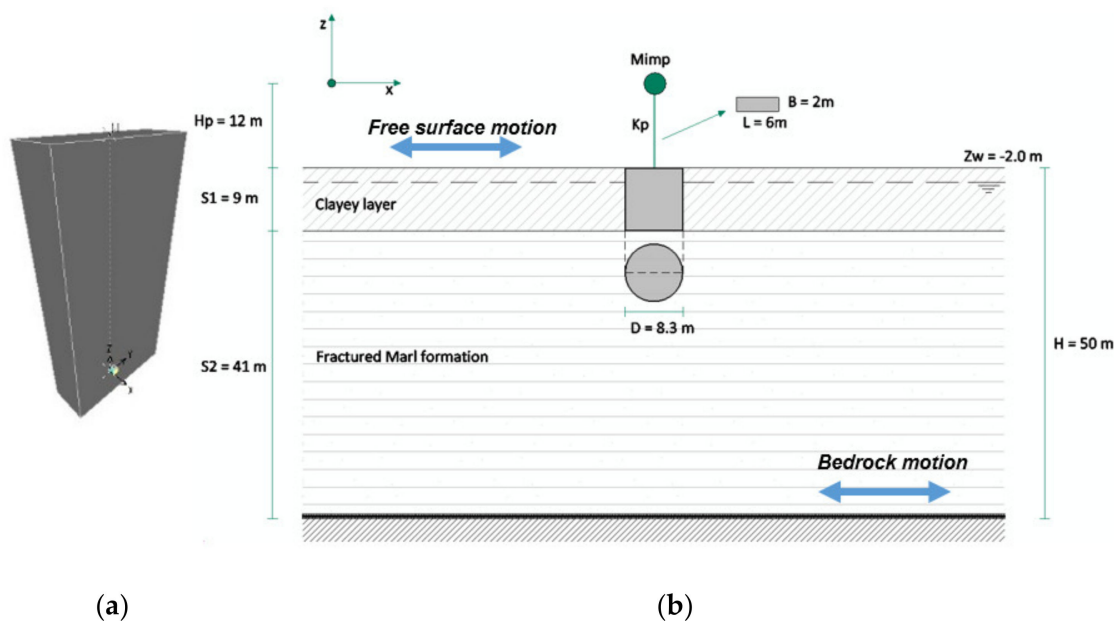


**Figure 4.** The Figure shows: (a) the 3D SAP 2000 model of the beam element fixed to the ground; (b) a sketch of the simplified geometry and soil layering.

The elastic modulus of the reinforced concrete pier is a non-cracked modulus (that is, the stiffness reduction due to cracking is not considered—this assumption will be the same for the PLAXIS 3D model, described in the following Section 4.2). The beam element is 12 m in height and its rectangular section is 6 m × 2 m. The dead load of the deck is applied by a nodal force at the top of the beam element and it is considered a mass source for the seismic analysis. To define the seismic input to apply to the bridge mass, a seismic site response analysis (SSRA) was performed, adopting the model shown in Figure 4b. Here, the considered stratigraphy is reported, along with the sketched geometrical characteristics of the model. The SSRA consisted of simulating the propagation of the seismic waves from the input base rock to the ground surface, assuming a non-linear constitutive model for the soil. For the SSRA, a 1D propagation analysis by means of the PLAXIS software and assuming a non-linear soil behavior (termed as *HS-small*) was performed.

#### 4.2. PLAXIS3D Model

Full dynamic numerical analyses were carried out with the PLAXIS3D FE software [44]. A 3D model—including the caisson, the pier, and the soil surrounding/underlying the caisson—was built. Figure 5 shows the geometry and mesh of the model. The considered soil volume is 100 m × 100 m wide, following Zaiferakos et al. [45] who suggest having a ratio between the horizontal dimension vs. the caisson diameter higher than 10, to have the lateral boundary sufficiently far from the structure and avoiding negative interferences due to reflection/refraction effects. To further reduce the effects produced by the presence of the boundaries, free field conditions were assumed at the lateral boundaries. They simulate the propagation of waves towards the far-field by minimizing the reflection at the lateral boundary. The bottom of the soil domain was fixed at 50 m and the hypothesis of a compliant base was assumed. This type of boundary condition simulates the propagation of seismic waves in the soil layers by minimizing their reflection at the bottom boundary. The entire soil domain was subdivided into 28,415 tetrahedral cluster elements with 10 nodes each.

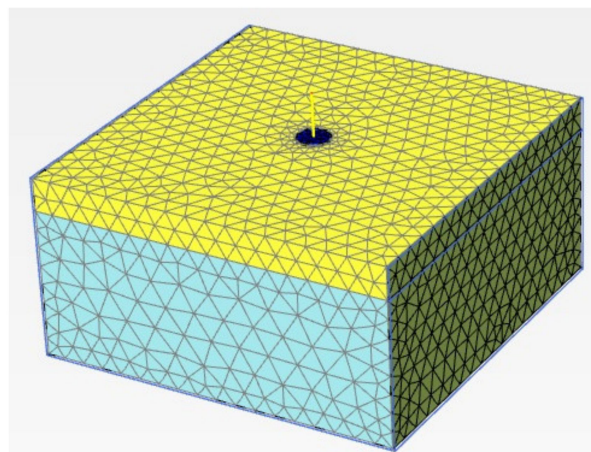


**Figure 5.** Three-dimensional FE model of the soil volume surrounding and underlining the examined pier.

The pier was modeled as a Timoshenko beam element of 12 m height and rectangular section of 6 m × 2 m. The caisson was modeled as a cylinder element of 8.3 m in diameter and 9 m in depth (Figure 6). Both these structural elements (pier and caisson) were modeled as linear visco-elastic elements, with a 5% damping ratio. The deck was modeled as a lumped mass of 4880 kN. Rigid interface elements between the foundation and soil were assumed. It should be noted that no interaction with surrounding bridge piers has been considered in the simulation to keep the model as simple as possible, yet realistic, to highlight the relevance of SSI effects. The goal of the simulation, indeed, is not that of assessing the safety conditions of the real structure, but to use a specific case study to explore the relevance of including the soil deformability in the dynamic analyses.

The stratigraphy was defined based on the detected depth of the Marl formation (at about 9 m from the surface). The stratigraphical contact between the two layers was assumed horizontal in the model, for the sake of simplicity and due to the limited volume considered. As shown in Figure 5, the soil volume was subdivided into two layers with different mechanical characteristics. The Marl formation was modeled using the Mohr–Coulomb elastoplastic constitutive model, and the dissipative behavior was considered using a damping ratio of 5%, as conducted, for example, by [23]. For the upper clayey layer, the constitutive model, called the Hardening Soil model, with small-strain stiffness (*HS small*) was adopted [44]. In contrast to a more traditional Hardening Soil model, the *HS small* shows hysteresis in cyclic loading. The amount of hysteresis depends on the magnitude of the corresponding strain amplitude. When applied in dynamics calculations, the hysteretic behavior of the *HS small* leads to damping. The amount of hysteretic damping depends on the applied load amplitude and corresponding strain amplitudes. The maximum amount of hysteretic damping obtained with the *HS small* depends on the ratio of  $G_0^{ref}$ , and  $G_{ur}^{ref} = E_{ur}^{ref} / 2(1 + \nu'_{ur})$ . A larger ratio leads to a larger maximum amount of hysteretic damping.

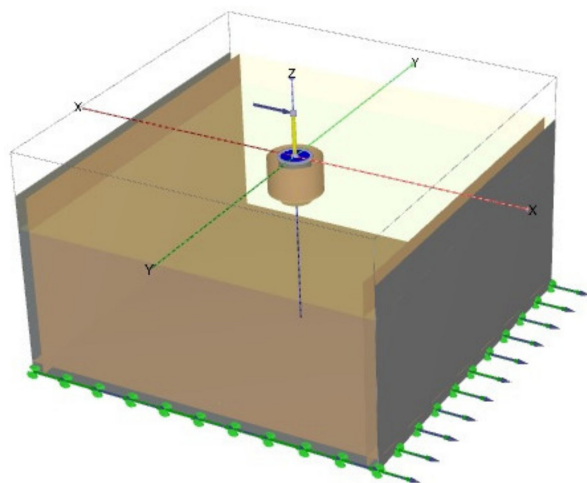


**Figure 6.** Three-dimensional view of the model, with the evidence of the caisson, modeled pier, and applied loads.

Table 2 shows the adopted soil properties, where the soil unit weight, cohesion, and friction angle derive from the technical reports of the original project, while the static and dynamic stiffness values ( $E_{50}^{ref}$ ;  $E_{oed}^{ref}$ ;  $E_{ur}^{ref}$ ,  $E'$ ,  $G_0^{ref}$ ,  $\gamma_{0.7}$ ,  $\nu'$ ) were adopted from literature values, considering documented cases of similar formations [46]. The meaning of the above parameters is the following:  $E_{50}^{ref}$  and  $E_{oed}^{ref}$  are secant stiffness in standard drained triaxial test and tangent stiffness for primary oedometer loading;  $E_{ur}^{ref}$  and  $E'$  are the unloading/reloading stiffness from drained triaxial test and the Young Modulus;  $G_0^{ref}$  and  $\gamma_{0.7}$  are the shear modulus at very small strains and the threshold shear strain at which  $G'_{sec} = 0.722G_0^{ref}$ ; and, finally,  $\nu'$  is the soil Poisson coefficient [40].

A set of numerical analyses was performed with PLAXIS-3D, to model the system response when considering the SSI, both in the case of free vibrations and when subjected to an earthquake (Section 3). First, the free vibration of the structure, after the application of a 1000 kN at the top of the pier, was evaluated, to numerically assess the structural period at small oscillations. Secondly, the seismic inputs described in Section 3 were applied at the bottom boundary of the FE model (with different  $F_a = 1.5, 1.0, 0.75,$  and  $0.4$ ). Results are shown in the following Section 5.

**Table 2.** Summary of the adopted soil properties.

Parameter	Symbol	Clayey F.	Marly F.	r.c.	Unit
Constit. model	-	HS-small	Mohr-Coulomb	Linear Elastic	-
Dry unit weight	$\gamma_s$	17	20	25/22	kN/m <sup>3</sup>
Sat unit weight	$\gamma_{sat}$	20	22		kN/m <sup>3</sup>
Mod. sec	$E'_{50}^{ref}$	20	-		MPa
Mod. tan	$E'_{oed}^{ref}$	20	-		MPa
Mod. unl/rel	$E'_{ur}^{ref}$	100	-		MPa
Young Modulus	$E'$	-	1350	30,000/25,000	MPa
Cohesion	$c'$	20	50	-	kN/m <sup>3</sup>
Friction angle	$\phi'$	25	28	-	°
Small-strain stiff.	$G'^{ref}_0$	150	-	-	MPa
Shear strain level	$\gamma_{0.7}$	$0.1 \times 10^{-3}$	-	-	-
Poisson coeff.	$\nu'$	0.25	0.35	0.2	-
Damp. Rayleigh	$\delta$	3%	5%	5%	-

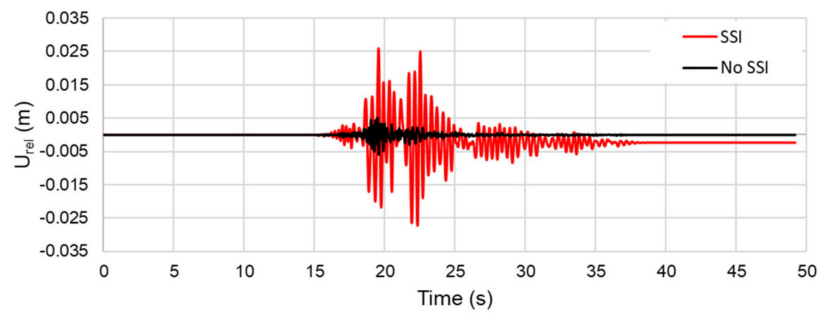
## 5. Results

To investigate the effects of the SSI on the pier behavior under seismic conditions, the results of the two FE models presented in Section 4.1 (where the pier was considered fixed to the base—and then the SSI was neglected) and Section 4.2 (where the pier was considered founded on a deformable soil—and the SSI was considered) have been compared. Model results are obtained in terms of:

- Natural periods under free vibrations and system period under seismic conditions, the latter computed as the period corresponding to the maximum value of the ratio between the pseudo-acceleration response spectrum with 5% damping at the top of the pier and the one at the base of the pier [47];
- Relative horizontal displacement ( $U_{rel}$ ) time-histories, evaluated as the difference between the absolute horizontal displacement at the top ( $U_{top}$ ) and base ( $U_{bas}$ ) of the pier;
- Rotation time-history of the pier;
- Moment and shear time-histories at the pier base.

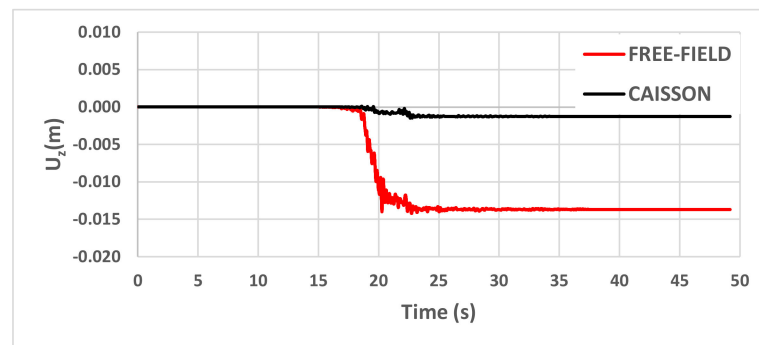
As for the natural periods of the pier, under free vibrations,  $T_{free-vib}$ , and system period under seismic conditions,  $T_{seismic}$ , the presence of a deformable soil produces a value of the  $T_{free-vib,SSI} = 0.29$  s, which is about double the one obtained under the hypothesis of rigid soil ( $T_{free-vib,FIX} = 0.148$  s). This value agrees with the simplified formulations by Tsigginos et al. [24] and the results of the parametric studies by De Angelis et al. [1]. Similar results have been obtained under seismic conditions: considering the SSI produces a value of the  $T_{seismic,SSI} = 0.37$  s, which is about 2.5 times the one obtained neglecting the SSI ( $T_{seismic,FIX} = 0.148$  s). This agrees with widely-known behaviors associated with the SSI effects, which elongate the natural period of the considered structure [10–12] and has an evident effect even for a stocky structure founded on a relatively rigid soil.

Figure 7 shows the comparison between the relative horizontal displacement time-histories obtained by the two models, for the seismic input n. 1 ( $F_a = 1.5$ ),  $U_{rel,1.5}$ . It is apparent that the presence of the SSI leads to a higher deformability of the system and, accordingly, the observed displacements are larger. Assuming the presence of a deformable pier-base, the maximum value of the relative horizontal displacement of the pier is  $U_{rel,1.5} = 0.027$  m, about 3.2 times higher than the one computed considering the fixed-base pier (see Table 3). The residual horizontal displacement at the top of the pier is  $U_{res,1.5} = 0.0024$  m considering the SSI, while it is null in the fixed-base case (Table 3).



**Figure 7.** Comparison between the relative horizontal displacement time-histories obtained by the two models, for the seismic input n. 1 ( $F_a = 1.5$ ).

To observe the variation of the deformation in the soil domain and examine the behavior in the *free-field* conditions compared to the one observed at the caisson foundation, the vertical displacements were computed at the caisson top and at about 30 m from the caisson, as shown in Figure 8. It can be observed that the presence of the foundation modifies the seismic response at the surface, since its inertia contribute to reduce the vertical displacements. Moreover, the smaller vertical displacement observed at the caisson are due to the design choice of embedding the foundation in the stiff Marly formation.



**Figure 8.** Comparison between the vertical displacement time-histories computed for the 3D model, at the caisson top, and in free-field conditions.

Table 3 shows the summary of the results obtained for the relative and residual horizontal displacement at the pier top for the four seismic inputs. A relevant effect of the SSI is apparent for all the four cases considered, with amplification of the horizontal relative displacement varying between 2.36 and 3.21. This amplification is quite similar for the three stronger seismic inputs, and decreases slightly for the weakest seismic input (n. 4). The same trend is also evident in Table 4, summarizing the results obtained in terms of horizontal displacements at the top ( $U_{top,k}$ ) and base ( $U_{bas,k}$ ) of the pier, for the four seismic inputs.

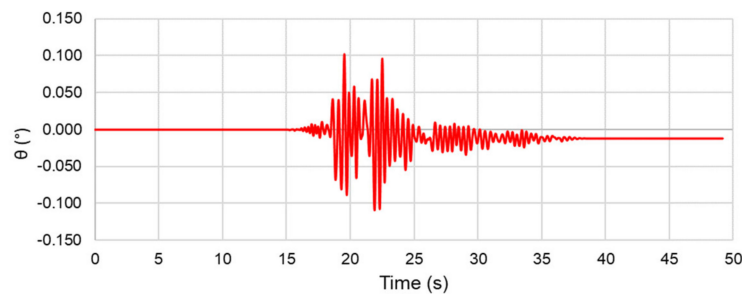
**Table 3.** Results obtained by the two models, considering and neglecting SSI, in terms of relative horizontal ( $U_{rel,k}$ ) and residual ( $U_{res,k}$ ) displacements of the pier, for the  $k$  seismic inputs.

	$U_{rel,1.5}$ (m)	$U_{rel,1.0}$ (m)	$U_{rel,0.75}$ (m)	$U_{rel,0.4}$ (m)	$U_{res,1.5}$ (m)	$U_{res,1.0}$ (m)	$U_{res,0.75}$ (m)	$U_{res,0.4}$ (m)
SSI	0.027	0.025	0.019	0.009	0.0024	0.0020	0.0012	0.0003
No-SSI	0.0084	0.0068	0.0058	0.0038	–	–	–	–
Ratio	3.21	3.67	3.27	2.36	–	–	–	–

**Table 4.** Results obtained by the two models, considering and neglecting SSI, in terms of horizontal displacements at: the top ( $U_{top,k}$ ) and base ( $U_{bas,k}$ ) of the pier, for the  $k$  seismic inputs.

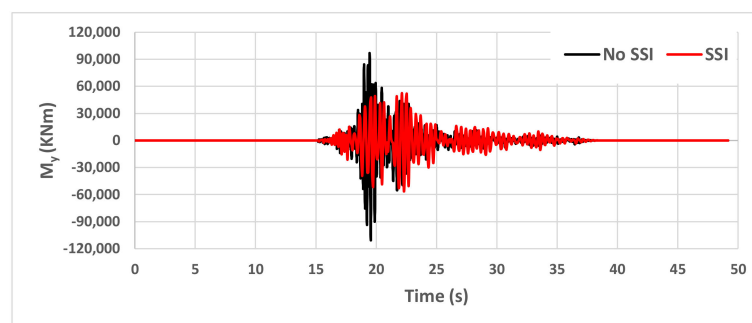
	$U_{top,1.5}$ (m)	$U_{top,1.0}$ (m)	$U_{top,0.75}$ (m)	$U_{top,0.4}$ (m)	$U_{bas,1.5}$ (m)	$U_{bas,1.0}$ (m)	$U_{bas,0.75}$ (m)	$U_{bas,0.4}$ (m)
SSI	0.078	0.059	0.048	0.021	0.057	0.040	0.032	0.016
No-SSI	0.0084	0.0068	0.0058	0.0038	–	–	–	–
Ratio	9.28	8.67	8.27	5.52	–	–	–	–

Figure 9 shows the rotation time-history due to SSI of the caisson for the seismic input n. 1 ( $F_a = 1.5$ ), which is obviously null in the fixed-base case. The maximum value obtained for the rotations is 0.002 rad for  $F_a = 1.5$ ; 0.0017 rad for  $F_a = 1$ ; 0.0012 rad for  $F_a = 0.75$ ; and 0.0003 rad for  $F_a = 0.4$ , decreasing, as expected, with the decreasing severity of the seismic input.



**Figure 9.** Rotation time-histories of the caisson, for the seismic input n. 1 ( $F_a = 1.5$ ).

The comparison between the moment time-histories at the pier base is shown in Figure 10 for the seismic input n. 1 (with  $F_a = 1.5$ ), both considering and neglecting the SSI. As predictable, considering the SSI leads to a  $M_{max}$  value which is lower than the corresponding value obtained with the embedded foundation (with a ratio of 0.35, as shown in Table 5). Similar ratios have been obtained considering all four seismic inputs (Table 5), varying between 0.35 and 0.45. In Table 6, a similar trend is shown for the maximum value of the shear at the pier base, again with a less sensitive decreasing for lower seismic inputs.



**Figure 10.** Comparison between the moment time-histories at the base of the pier obtained by the two models, considering or neglecting the SSI, for the seismic input n. 1 ( $F_a = 1.5$ ).

**Table 5.** Maximum moments computed by including vs. neglecting SSI, for the four seismic inputs.

	$M_{max,1.5}$ (kNm)	$M_{max,1.0}$ (kNm)	$M_{max,0.75}$ (kNm)	$M_{max,0.4}$ (kNm)
SSI	56,053	55,475	50,895	32,652
No-SSI	159,100	129,800	109,500	71,620
Ratio	0.35	0.42	0.46	0.45

**Table 6.** Shear at the pier base computed by including vs. neglecting SSI, for the four seismic inputs.

	$V_{\max,1.5}$ (kN)	$V_{\max,1.0}$ (kN)	$V_{\max,0.75}$ (kN)	$V_{\max,0.4}$ (kN)
SSI	5097	5068	4911	3074
No-SSI	13,260	10,820	9126	5209
Ratio	0.38	0.46	0.53	0.59

## 6. Conclusions and Perspectives

Two FE models have been used to evaluate the importance of soil–structure interaction phenomena on the response of a reinforced concrete bridge pier founded on a caisson under different seismic conditions. The comparison between the results obtained considering a deformable foundation soil and those obtained considering an infinitely rigid soil has allowed quantitative evaluation of the influence of SSI, both in the field of small deformations and in the case of strong motion events.

As observed by [11], considering soil deformability in the soil–foundation system can lead either to a reduction or to an increase in the computed forces on the structure, depending on the characteristics of the response spectrum of the considered seismic input. For the considered case study, the effect of SSI is beneficial in terms of shear forces and bending moments, which are reduced up to 38% and by about 45% on average compared to the rigid soil case. However, the increase in the deformability of the system has a significant impact on the deck displacements (evaluated at the pier top): with a maximum value of the relative horizontal displacement that is up to 3.2 times higher than in the rigid case. Although the SSI topic has been widely studied recently, applications to new case studies, as the one presented in this paper, allow emphasizing the relevance of the phenomenon even for cases of: (i) relatively stiff subsoil (as the considered Marly formation) and (ii) low-intensity seismic inputs. Further perspectives of this work will consider the influence of other parameters affecting the SSI, such as: stiffness and resistance interface element, different soil constitutive models, and different seismic inputs in terms of frequency content. Future perspectives also include extensions of the comparison considering nonlinearities in the structure behavior, along with structure dissipative capacities through advanced techniques of multimodal pushover analyses [48,49].

**Author Contributions:** Conceptualization, D.P., D.S. and F.U.; Data curation, D.P.; Formal analysis, D.P.; Methodology, D.P., D.S. and F.U.; Software, D.P.; Supervision, D.S. and F.U.; Writing—original draft, D.P.; Writing—review & editing, D.S. and F.U. All authors have read and agreed to the published version of the manuscript.

**Funding:** This research received funding from the Italian FABRE Consortium ([www.consortziofabre.it](http://www.consortziofabre.it)) through the grant entitled “Multilevel Safety Analysis and Monitoring of Existing Bridges” (2021–2022).

**Institutional Review Board Statement:** Not applicable.

**Informed Consent Statement:** Not applicable.

**Data Availability Statement:** Not applicable.

**Acknowledgments:** The collaboration of the National Autonomous Roads Corporation (ANAS), which provided technical information about the case study bridge, is gratefully acknowledged.

**Conflicts of Interest:** The authors declare no conflict of interest. The funders had no role in the design of the study; in the collection, analyses, or interpretation of data; in the writing of the manuscript; or in the decision to publish the results.

## References

- De Angelis, A.; Mucciacciaro, M.; Pecce, M.R.; Sica, S. Influence of SSI on the Stiffness of Bridge Systems Founded on Caissons. *J. Bridge Eng.* **2017**, *22*, 4017045. [[CrossRef](#)]
- Gerolymos, N.; Gazetas, G. Static and dynamic response of massive caisson foundations with soil and interface nonlinearities—validation and results. *Soil Dyn. Earthq. Eng.* **2006**, *26*, 377–394. [[CrossRef](#)]

3. Gerolymos, N.; Gazetas, G. Winkler model for lateral response of rigid caisson foundations in linear soil. *Soil Dyn. Earthq. Eng.* **2006**, *26*, 347–361. [[CrossRef](#)]
4. Varun; Assimaki, D.; Gazetas, G. A simplified model for lateral response of large diameter caisson foundations—Linear elastic formulation. *Soil Dyn. Earthq. Eng.* **2009**, *29*, 268–291. [[CrossRef](#)]
5. Zafeirakos, A.; Gerolymos, N.; Gazetas, G. The role of soil and interface nonlinearities on the seismic response of caisson supported bridge piers. In Proceedings of the 5th International Conference on Geotechnical Earthquake Engineering, Santiago, Chile, 13 January 2011.
6. Buscarnera, G.; Nova, R.; Vecchiotti, M.; Tamagnini, C.; Salciarini, D. Settlement analysis of wind turbines. In *Soil-Foundation-Structure Interaction*; CRC Press: Boca Raton, FL, USA, 2010; pp. 163–170.
7. Grange, S.; Salciarini, D.; Kotronis, P.; Tamagnini, C. A comparison of different approaches for the modelling of shallow foundations in seismic soil-structure interaction problems. In *Numerical Methods in Geotechnical Engineering, Proceedings of the 7th European Conference on Numerical Methods in Geotechnical Engineering, Trondheim, Norway, 2–4 June 2010*; CRC Press: Boca Raton, FL, USA, 2010; pp. 405–410.
8. Venanzi, I.; Salciarini, D.; Tamagnini, C. The effect of soil–foundation–structure interaction on the wind-induced response of tall buildings. *Eng. Struct.* **2014**, *79*, 117–130. [[CrossRef](#)]
9. Salciarini, D.; Frizza, M.; Tamagnini, C.; Arroyo, M.; Abadías, D. Macroelement Modeling of SSI Effects on Offshore Wind Turbines Subject to Large Number of Loading Cycles. *Procedia Eng.* **2016**, *158*, 332–337. [[CrossRef](#)]
10. Gazetas, G. *Foundation Vibrations, Foundation Engineering Handbook*; Fang, H.Y., Ed.; Van Nostrand Reinhold: New York, NY, USA, 1991; Chapter 15; pp. 553–592.
11. Mylonakis, G.; Gazetas, G. Seismic soil-structure interaction: Beneficial or detrimental? *J. Earthq. Eng.* **2000**, *4*, 277–301. [[CrossRef](#)]
12. Wolf, J.P. *Soil Structure Interaction*; Englewood Cliffs, N.J., Ed.; Prentice-Hall: Hoboken, NJ, USA, 1985.
13. Chellini, G.; Nardini, L.; Salvatore, W. Dynamical identification and modelling of steel-concrete composite high-speed railway bridges. *Struct. Infrastruct. Eng.* **2011**, *7*, 823–841. [[CrossRef](#)]
14. Gara, F.; Regni, M.; Roia, D.; Carbonari, S.; Dezi, F. Evidence of coupled soil-structure interaction and site response in continuous viaducts from ambient vibration tests. *Soil Dyn. Earthq. Eng.* **2019**, *120*, 408–422. [[CrossRef](#)]
15. Marrongelli, G.; Gentile, C.; Saisi, A. Anomaly Detection Based on Automated OMA and Mode Shape Changes: Application on a Historic Arch Bridge Structural Integrity. In *International Conference on Arch Bridges*; Springer: Cham, Switzerland, 2020; Volume 11, pp. 447–455.
16. Zampieri, P.; Simoncello, N.; Gonzalez-Libreros, J.; Pellegrino, C. Evaluation of the vertical load capacity of masonry arch bridges strengthened with FRCM or SFRM by limit analysis. *Eng. Struct.* **2020**, *225*, 111135. [[CrossRef](#)]
17. Ciampoli, M.; Pinto, E. Effects of soil-structure interaction on inelastic seismic response of bridge piers. *J. Struct. Eng.* **1995**, *121*, 806–814. [[CrossRef](#)]
18. Dicleli, M.; Lee, J.Y.; Mansour, M. Importance of soil-bridge interaction modeling in seismic analysis of seismic-isolated bridges. In Proceedings of the 13th World Conference on Earthquake Engineering, Vancouver, BC, Canada, 1–6 August 2004.
19. Jeremic, B.; Kunnath, S.; Xiong, F. Influence of soil foundation-structure interaction on seismic response of the I-880 viaduct. *Eng. Struct.* **2004**, *26*, 391–402. [[CrossRef](#)]
20. Makris, N.; Badoni, D.; Delis, E.; Gazetas, G. Prediction of observed bridge response with soil-pile-structure interaction. *J. Struct. Eng.* **1995**, *120*, 2992–3011. [[CrossRef](#)]
21. Veletsos, A.S.; Meek, J.W. Dynamic behaviour of building-foundation systems. *Earthq. Eng. Struct. Dyn.* **1974**, *3*, 121–138. [[CrossRef](#)]
22. Gaudio, D.; Rampello, S. The influence of soil plasticity on the seismic performance of bridge piers on caisson foundations. *Soil Dyn. Earthq. Eng.* **2019**, *118*, 120–133. [[CrossRef](#)]
23. Mucciacciaro, M.; Gerolymos, N.; Sica, S. Seismic response of caisson-supported bridge piers on viscoelastic soil. *Soil Dyn. Earthq. Eng.* **2020**, *139*, 106341. [[CrossRef](#)]
24. Tsigginos, C.; Gerolymos, N.; Assimaki, D.; Gazetas, G. Seismic response of bridge pier on rigid caisson foundation in soil stratum. *Earthq. Eng. Vib.* **2008**, *7*, 33–43. [[CrossRef](#)]
25. Lai, C.G.; Martinelli, M. Soil-Structure Interaction Under Earthquake Loading: Theoretical Framework. *ALERT Dr. Sch. Soil-Struct. Interact.* **2013**, *2013*, 3–43.
26. Salciarini, D.; Grange, S.; Tamagnini, C.; Kotronis, P. Macroelements for Soil–Structure Interaction. In *Deterministic Numerical Modeling of Soil Structure Interaction*; Grange, S., Salciarini, D., Eds.; ISTE: London, UK; Wiley: Oxford, UK, 2022.
27. Mylonakis, G.; Nikolaou, A. Soil-Pile-Bridge Seismic Interaction: Kinematic and Inertial Effects. Part I: Soft Soil. *Earthq. Eng. Struct. Dyn.* **1997**, *26*, 337–359. [[CrossRef](#)]
28. Mylonakis, G.; Nikolaou, S.; Gazetas, G. Footings under seismic loading: Analysis and design issues with emphasis on bridge foundations. *Soil Dyn. Earthq. Eng.* **2006**, *26*, 824–853. [[CrossRef](#)]
29. Wolf, P.W. *Foundation Vibration Analysis Using Simple Physical Models*; Pearson Education: London, UK, 1994; p. 464.
30. Davies, T.G.; Budhu, M. No Access Non-linear analysis of laterally loaded piles in heavily overconsolidated clays. *Géotechnique* **1986**, *36*, 527–538. [[CrossRef](#)]
31. Pender, M.J. Earthquake resistant design of foundations. *Bull. N. Z. Soc. Earthq. Eng.* **1996**, *29*, 155–171. [[CrossRef](#)]
32. Nova, R.; Montrasio, L. Settlements of shallow foundations on sand. *Geotechnique* **1991**, *41*, 243–256. [[CrossRef](#)]

33. Tamagnini, C.; Salciarini, D.; Ragni, R. Implementation of a 6-DOF hypoplastic macroelement in a finite element code. In *Computational Geomechanics, COMGEO III, Proceedings of the 3rd International Symposium on Computational Geomechanics, Krakow, Poland, 21–23 August 2013*; International Centre for Computational Engineering: Rhodes, Greece, 2013; pp. 534–544. Available online: <http://www.ic2e.org/wp-content/uploads/2019/03/Proceedings-ComGeo-3.pdf> (accessed on 27 September 2022).
34. Salciarini, D.; Bienen, B.; Tamagnini, C. Incorporating scale effects in shallow footings in a hypoplastic macroelement model. In *Numerical Methods in Geotechnical Engineering, Proceedings of the 8th European Conference on Numerical Methods in Geotechnical Engineering, NUMGE 2014, Delft, The Netherlands, 18–20 Jun 2014*; CRC/Balkema: Leiden, The Netherlands, 2014; Volume 1, pp. 397–402.
35. Grange, S. Simplified modeling strategies for soil-structure interaction problems: The Macro-Element Concept. *ALERT Dr. Sch. Soil-Struct. Interact.* **2013**, *2013*, 195–217.
36. Ritesh, G. Behaviour of Monopile Under Combined Cycling Load. Ph.D. Thesis, Université Grenoble Alpes, Grenoble, France, 2020.
37. Salciarini, D.; Bienen, B.; Tamagnini, C. A hypoplastic macroelement for shallow foundations subject to six-dimensional loading paths. In *Computational Geomechanics, COMGEO II, Proceedings of the 2nd International Symposium on Computational Geomechanics, Dubrovnik, Croatia, 27–29 April 2011*; International Centre for Computational Engineering: Rhodes, Greece, 2011; pp. 721–733.
38. Kita, A.; Lupattelli, A.; Venanzi, I.; Salciarini, D.; Ubertini, F. The role of seismic hazard modeling on the simplified structural assessment of an existing concrete gravity dam. *Structures* **2021**, *34*, 4560–4573. [[CrossRef](#)]
39. Breccolotti, M.; Materazzi, A.L.; Salciarini, D.; Tamagnini, C.; Ubertini, F. Vibrations induced by the new underground railway line in Palermo, Italy: Experimental measurements and FE modeling. In *Proceedings of the 8th International Conference on Structural Dynamics, EURODDYN 2011, Leuven, Belgium, 4–6 July 2011*; pp. 719–726.
40. Cattoni, E.; Salciarini, D.; Tamagnini, C. A Generalized Newmark Method for the assessment of permanent displacements of flexible retaining structures under seismic loading conditions. *Soil Dyn. Earthq. Eng.* **2018**, *117*, 221–233. [[CrossRef](#)]
41. Kozielova, M.; Marcalikova, Z.; Mateckova, P.; Sucharda, O. Numerical Analysis of Reinforced Concrete Slab with Subsoil. *Civ. Environ. Eng.* **2020**, *16*, 107–118. [[CrossRef](#)]
42. Iervolino, I.; Galasso, C.; Cosenza, E. REXEL: Computer aided record selection for code-based seismic structural analysis. *Bull. Earthq. Eng.* **2009**, *8*, 339–362. [[CrossRef](#)]
43. *SAP2000 [Computer Software]*; Computers & Structures, Inc.: Walnut Creek, CA, USA, 2000.
44. *Plaxis 3D Foundation [Computer Software]*; Bentley: Crewe, UK, 2000.
45. Zafeirakos, A.; Gerolymos, N. On the seismic response of under-designed caisson foundations. *Bull. Earthq. Eng.* **2013**, *11*, 1337–1372. [[CrossRef](#)]
46. Kulhawy, F.H.; Mayne, P.W. *Manual on Estimating Soil Properties for Foundation Design*; Cornell University: Ithaca, NY, USA, 1990.
47. Elia, G.; Rouinia, M. Seismic Performance of Earth Embankment Using simple and advanced numerical approaches. *J. Geotech. Geoenviron. Eng.* **2013**, *139*, 115–1129. [[CrossRef](#)]
48. Crespi, P.; Zucca, M.; Longarini, N.; Giordano, N. Seismic Assessment of Six Typologies of Existing RC Bridges. *Infrastructures* **2020**, *5*, 52. [[CrossRef](#)]
49. Yazdani, M.; Jahangiri, V.; Merefat, M.S. Seismic performance assessment of plain concrete arch bridges under near-field earthquakes using incremental dynamic analysis. *Eng. Fail. Anal.* **2019**, *106*, 104170. [[CrossRef](#)]